Journal of Minerals and Materials Characterization and Engineering, 2025, 13(4), 107-122
https://www.scirp.org/journal/jmmce
ISSN Online: 2327-4085
ISSN Print: 2327-4077

Correlation between Surface OH^- Groups and Fractal Dimensions of Synthetic Boehmite, Goethite, and Manganite: Insights into Their Physical-Adsorbent Properties

Francisco Granados-Correa*, Melania Jiménez-Reyes

Departamento de Química, Gerencia de Ciencias Básicas, Instituto Nacional de Investigaciones Nucleares, Ocoyoacac, México
Email: *francisco.granados@inin.gob.mx, melaniajr51@gmail.com

How to cite this paper: Granados-Correa, F. and Jiménez-Reyes, M. (2025) Correlation between Surface OH^- Groups and Fractal Dimensions of Synthetic Boehmite, Goethite, and Manganite: Insights into Their Physical-Adsorbent Properties. *Journal of Minerals and Materials Characterization and Engineering*, **13**, 107-122.
https://doi.org/10.4236/jmmce.2025.134008

Received: May 21, 2025
Accepted: July 1, 2025
Published: July 4, 2025

Abstract

The oxyhydroxides boehmite, goethite, and manganite were synthesized, and their structure, texture, and morphology features were determined by different analytical techniques. Content of surface hydroxyl groups and zero point of charge (pH_{zpc}) were measured by potentiometry, and the surface fractal dimension (D_f) values were obtained through adsorption-desorption N_2 isotherms and the Pfeifer and Cole method. The synthesized materials resulted crystalline, mesoporous, pure, and thermally stable, exhibiting high surface areas, between 188 and 413 m^2/g. The pH_{zpc} values were 9.2, 12.4, and 2.2 and surface hydroxyl group contents were for 1.16, 1.7, and 0.855 meq OH^-/g, for boehmite, goethite, and manganite, respectively. Surface fractal dimensions were 1.5, 1.7, and 1.4 for boehmite, goethite and manganite, respectively, denoting relatively smooth surfaces. Surface hydroxyl group content linearly correlated with D_f values. Characterization of these oxyhydroxides is valuable for several physicochemical adsorption processes of contaminants present in aqueous media.

Keywords

Oxyhydroxides, Synthesis, Characterization, Surface Fractal Dimensions, Surface Hydroxyl Groups

1. Introduction

Diverse conventional wastewater treatments, have been used in recent years for mitigation of water pollution caused by a vast gamma of environmentally unde-

sirable and potentially toxic elements. The adsorption onto solid adsorbents has been the most employed technology, due to low cost and ease operation [1]. A wide variety of natural and synthetic solid adsorbents with different chemical, structural, and surface characteristics have been extensively studied in terms of their adsorption behavior [2] [3]. The surface properties of the adsorbents impact on the removing of toxics elements, nuclear or not, from aqueous media [4] and surface area, zero charge point, hydroxyl groups and porosity are among these key properties; however, the fractal dimension (roughness) as superficial property of solids has been little studied for adsorption purposes. So, this pioneering study allows looking for a new and important approach on this interesting surface property of solid adsorbents.

Roughness can be understood as the set of atomic irregularities of a surface, and the value of the fractal dimension parameter (D_f) is closely related to the roughness profile of a powder material. The roughness of the surface is due to the presence of uniform size pores or to distribution of larger pore size [5]. Measurements of this parameter are achieved by diverse methods, N_2 physisorption on powders is one of them. Values of D_f below 2 indicate regularity and smoothness of surfaces, whereas values close to 3 reveal irregular or rough surfaces [6]. Many determinations of fractal dimension (D_f) studies have been carried out involving the heterogeneity of the structural geometry of solid surfaces [7]-[11]; particularly, fractal dimension of building materials has gained attention recently [12]-[16]. The surface fractal dimension values are useful for understanding several physicochemical processes (adsorption, adhesion, surface diffusion and catalyst) because the structural heterogeneity of solids affects their interaction with other substances [17] [18]. Contreras-Ruiz *et al.* (2016) [18] determined D_f of TiO_2-Hydrotalcite composites and these mesoporous materials were in the intermediate roughness range ($2.11 \leq D_f \leq 2.47$). Vilchis-Granados *et al.* (2013) [19] examined the surface fractal dimensions (D_f) and textural properties of three different alkaline-earth hydroxyapatites. They found that the D_f values for these materials range from 0.7 to 2.3 and reported a linear correlation between the surface hydroxyl group content and the surface fractal dimensions. On other hand, some studies included a relationship between D_f dimensions of adsorbent materials and adsorption mechanism regarding aqueous decontamination [19] [20].

The oxyhydroxides of the present study occur in soils, rocks, and sediments [21] where they are crystalline in nature; but when synthesized the crystallinity depends upon the preparation method [22]. Recently these compounds have shown being a considerable promise in environmental remediation, due to their chemical, surface, and structural properties [22]. Structurally, boehmite (γ-AlOOH) consists of $Al(O,OH)_6$ octahedral layers [22]. Goethite (α-FeOOH) is one of the most common oxyhydroxide and the structure includes FeO_6 octahedral units liked by corners, edges, or faces, so forming different structural arrays that remain even in amorphous state [23]. Manganite (γ-MnOOH) is composed of octahedral units of $Mn^{3+}O_6$ that are edge and corner-shared forming a 1×1 tunnel

in which hydrogen atoms reside [24]. The synthetic oxyhydroxides have a variety of technical applications, to mention a few, in pigments, electrochemical reactions, electrochromic materials, lithium batteries, and catalysis [25]. Adsorption capacities of these oxyhydroxides have also been studied regarding decontamination of aqueous solutions [26]-[28] and resulted in good adsorbents due to their high surface areas, surface reactivity, resistance to high temperature and radiation, structural flexibility, and relatively low cost.

The aim of this study was to evaluate the properties of the oxyhydroxides boehmite, goethite, and manganite, synthesized from different processing methods. Techniques such as XRD. SEM-EDS, FTIR, TGA-DSC, potentiometry, and N_2 physisorption isotherms allowed determining data on surface area, mean pore diameter, total pore volume, surface hydroxyl groups, zero point of charge, grain size, purity, thermo-stability, crystallinity, and surface fractal dimension. The relationship between that last parameter and the hydroxyl group content of these materials was explored.

2. Experimental

2.1. Synthesis of Oxyhydroxides

All chemicals used in this study came from commercial sources, were of analytical grade and used as received without further purification. Solutions were prepared with deionized water.

Boehmite was synthesized by a sol-gel method [29]. An isopropanol-water solution was slowly added into a 0.5 M aluminum isopropoxide/isopropanol solution, and thereafter the mixture was stirred for 30 minutes at room temperature. The resulting gel was aged at 25˚C for 24 hours, separated by centrifugation, washed with abundant deionized water, and finally dried for 12 hours at 60˚C. Goethite was obtained by the Fe (II) hydrolysis method [30], using 0.5 M $FeSO_4{\cdot}7H_2O$ and 0.2 M NaOH solutions. These precursors were under constant stirring for 20 hours at room temperature and the obtained precipitate was washed, subsequently dried at 50˚C, and ground using an agate mortar. Manganite was prepared by the Mn (II) oxidizing method [31], which consists in mixing 0.06 M $MnSO_4{\cdot}H_2O$, 0.2 M NH_3, and 30% H_2O_2, aqueous solutions under vigorous stirring, at 95˚C for 6 hours. The precipitate was filtered, washed with deionized water, and dried at 50˚C.

2.2. Characterization of Materials

X-ray diffraction spectra were recorded by using a Siemens D-5000 diffractometer coupled to a copper anode tube. A beam monochromator allowed to select the *Kα* wavelength and diffractograms were obtained in a step-scanning mode (0.02˚ for 3 s) from five to 70 2θ angle. The Joint Committee on Powder Diffraction Standards (JCPDS) files were used to identify the phases of the oxyhydroxides by the conventional method. The morphology and chemical elemental composition were revealed by means of a scanning electron microscope (JEOL JMS-5900 LV) with

an EDS (energy X-ray dispersive spectroscopy) microprobe. Fourier transformer infrared spectra were obtained with a Nicolette IR 550 spectrophotometer, for which oxyhydroxide samples were mixed with KBr and following the usual method. Thermogravimetric and differential scanning calorimetric analysis were performed into a temperature range of 25˚C to 1000˚C at a heating rate of 10˚C/min and under air atmosphere with a SDT Q600 TA Instrument-Waters calorimeter. The zero point of charge (pH_{zpc}) was determined putting in contact for 24 h 100 mg of sample and 0.1 M sodium nitrate solutions of pH from 2 to 10. After separation, pH of the supernatant was measured with a digital pH-meter (Cole-Parmer potentiometer model 05669-20), using a combined glass electrode [32]. The plot of ΔpH ($pH_{initial} - pH_{final}$) vs. $pH_{initial}$ (figure not included) presented linearity and pH_{zpc} was obtained at $\Delta pH = 0$. The content of the surface hydroxyl group of each material was evaluated by means of acid/base potentiometric titrations [33]. Physical N_2 adsorption isotherms were determined at room temperature with a physisorption equipment Belsorp BEL Japan Inc. Max; all samples were previously degasified at 200˚C for 2 hours in vacuum. Brunauer-Emmet-Teller (BET) surface areas, total pore volumes, mean pore diameters, and surface fractal dimensions (D_f) were evaluated by means of these measurements. The last parameters were calculated from data of isotherms and the theory of Pfeifer and Cole (1990) [6].

3. Results and Discussions

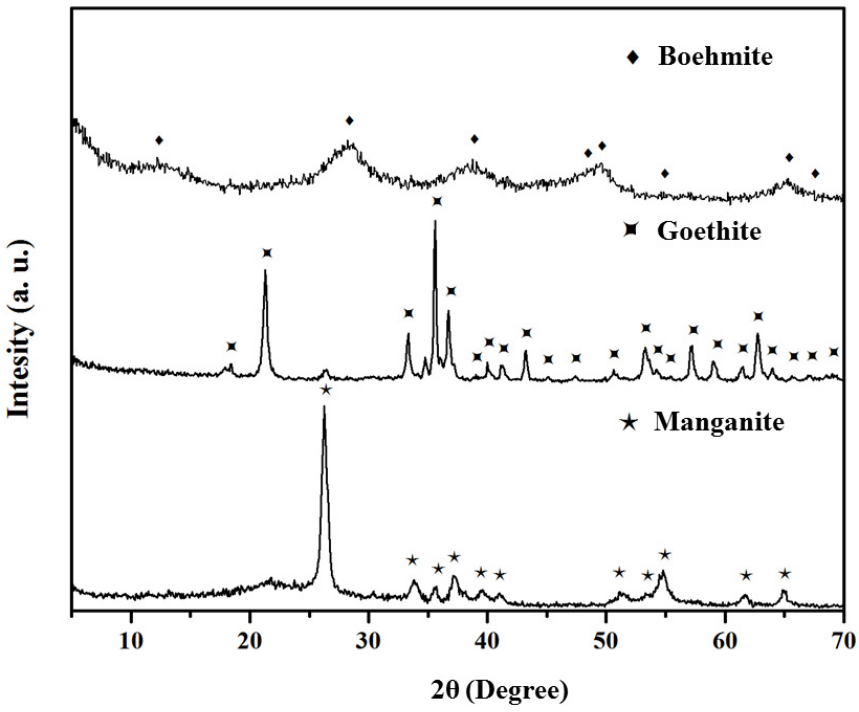

Figure 1. X-ray diffraction patterns of synthesized oxyhydroxides.

The XRD patterns of the synthesized oxyhydroxides are shown in (Figure 1).

The boehmite powder synthesized by the sol-gel method presents peaks associated with the amorphous phase of γ-AlOOH (JCPDS card 21-1307); this result agrees with those found elsewhere [22] [34]. On the contrary, hydrolysis and oxidizing methods used for goethite and manganite, respectively, resulted in crystalline phases. The goethite diffractogram (**Figure 1**) showed the phase of α-FeOOH (JCPDS card 81-0462) in agreement with Brigante *et al.* 2010 [35], and Granados-Correa *et al.* 2011 [27]. **Figure 1** showed as well the manganite diffractogram, corresponding to the phase of the γ-MnOOH (JCPDS card 41-1379), resulting like that reported by Chen *et al.* 2009 [36].

Figure 2 shows the micrographs at 100x of the synthesized oxyhydroxides. The boehmite powder (**Figure 2(a)**) consists of irregular, smooth-surfaced grains with particle sizes between 10 and 200 μm. Goethite powder (**Figure 2(b)**), appears as irregular, large, and agglomerated particles, each grain of which is composed of very porous and fine particles of about 40 to 500 μm in size. The SEM examination of manganite powders (**Figure 2(c)**) showed flakes of irregular sharpness with a wide range of sizes, from 30 to 400 μm. EDX analysis of the oxyhydroxides revealed the presence of the characteristic metal of each material: in boehmite 29% Al, in goethite 61% Fe, and in manganite 65% Mn. The aluminum percentage of the synthesized boehmite is lower than expected by its chemical formula (45%). Alternatively, the experimental values of the metallic content of the two last materials are near to those of goethite and manganite (63% and 62% for iron and manganese, respectively). These differences may be imputed by synthesis methods.

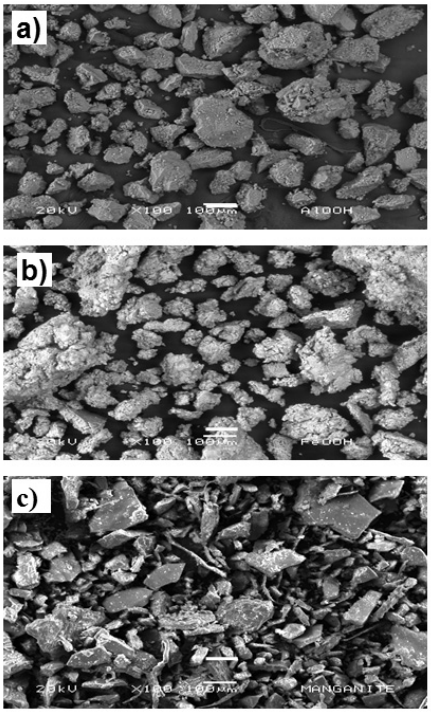

Boehmite		
Element	**Element (%)**	**Atomic (%)**
C	26.20	36.06
O	44.53	46.00
Al	29.26	17.92

Goethite		
Element	**Element (%)**	**Atomic (%)**
C	19.80	41.68
O	19.51	30.83
Fe	60.68	27.47

Manganite		
Element	**Element (%)**	**Atomic (%)**
C	5.31	12.71
O	29.66	53.27
Mn	65.02	34.01

Figure 2. SEM images at 100× and EDX data. (a) Boehmite, (b) Goethite, and (c) Manganite.

Figure 3 shows the FTIR spectra of the oxyhydroxides; all of them show a strong band at around 3400 cm^{-1} related to the stretching vibration of H_2O molecules or to the surface OH groups and additionally a band around 1600 cm^{-1} is due to the OH groups [37]. The main bands of boehmite (Figure 3(a)) at 611 and 482 cm^{-1}, are attributed to the reflection in the angular plane OH-Al=O, while the band at 1072 cm^{-1} corresponds to symmetric and asymmetric bending of AlOH [38]. For goethite (Figure 3(b)), the major bands are at 399 and 635 cm^{-1}, caused by Fe-O and Fe-O-OH bonds and in addition the bands at 796, and 839 cm^{-1} correspond to OH^- groups [37]. Manganite spectrum (Figure 3(c)) shows peaks at 364, 447, 489, and 594 cm^{-1} of the Mn-O vibrations [39], the absorption band at around 2100 cm^{-1} and those around 1000 cm^{-1} - 1200 cm^{-1} can be attributed to O-H modes, like γ-OH, δ-2-OH, and δ-1-OH [21].

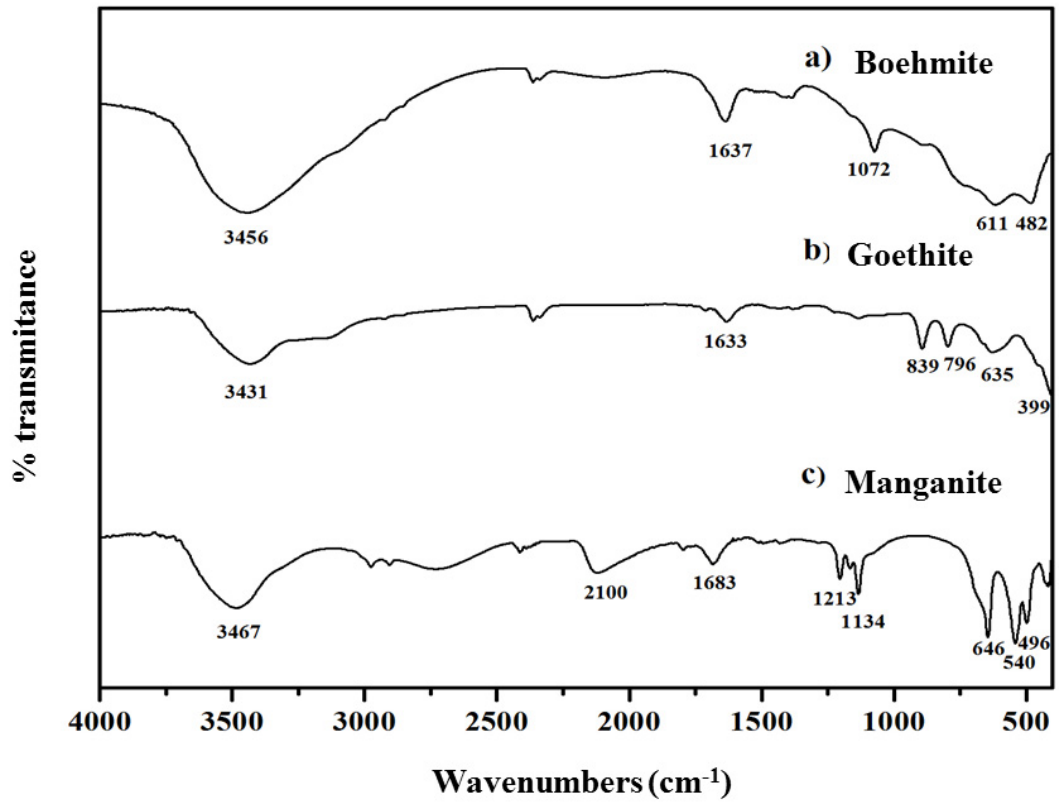

Figure 3. FTIR spectra of synthesized oxyhydroxides.

Figure 4 shows the TGA-DSC curves of boehmite, goethite, and manganite powders. The boehmite TGA curve (Figure 4(a)) shows three weight loss steps. The first significant one (24.2%) is due to the water evaporation contained in the sample and was between 10˚C - 210˚C [40] with an endothermic peak at 88˚C. The second one (7.0%) occurred at 210˚C - 390˚C and corresponds to the material dihydroxylation. Finally, the third weight loss (4.9%) was at 390˚C - 550˚C (endothermic peak at 400˚C), attributable to a structural conversion from γ-AlOOH to γ-Al_2O_3 [41] [42].

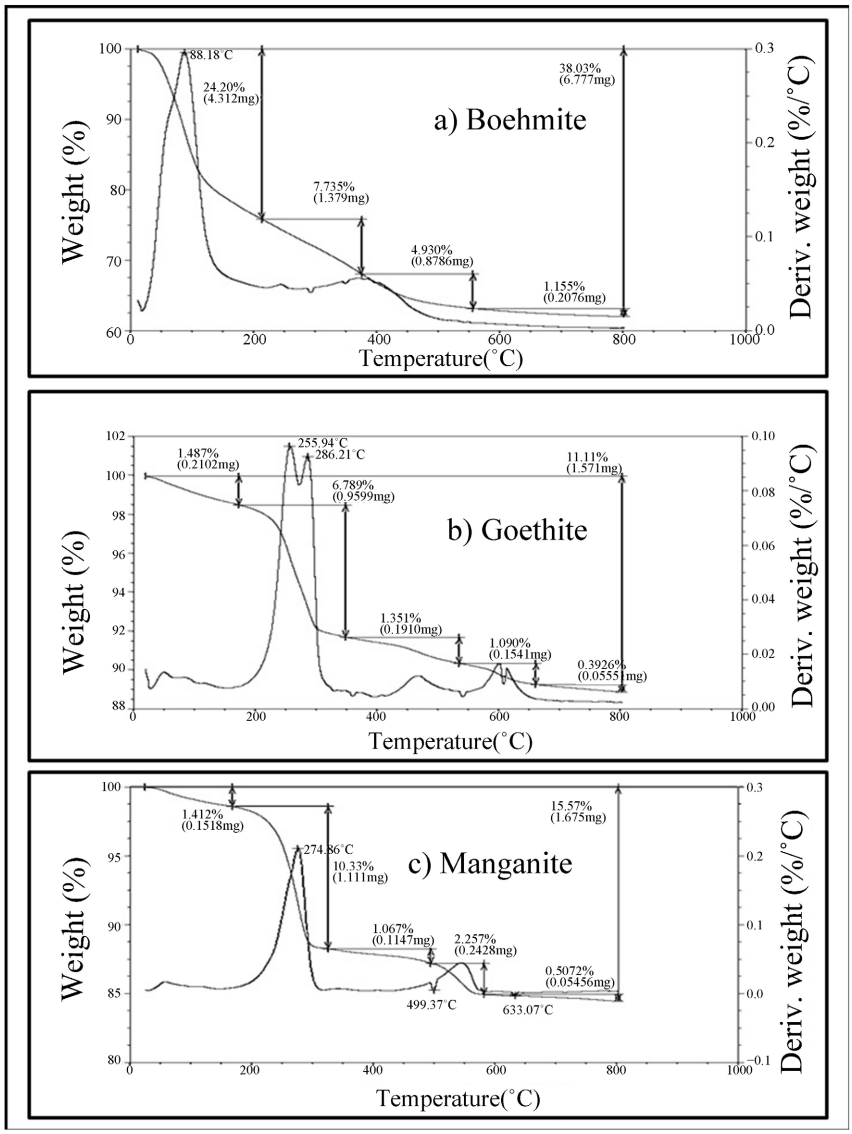

Figure 4. TGA-DSC curves of as-prepared boehmite, goethite, and manganite powders.

The goethite TGA curve (**Figure 4(b)**) shows a 1.48% weight loss between 10 to 160˚C due to the physical desorption of water and a second one (6.78%) upon heating to 160˚C. A third weight loss occurs at a temperature range of 350˚C - 540˚C due to the loss of structural hydroxyl groups [43]. The DSC curve (**Figure 4(b)**) shows several endothermic peaks. The first ones at 255.9 and 286.2˚C are due to dehydration and the conversion of goethite (α-$Fe^{3+}O$ (OH)) into hematite ($(Fe^{3+})_2O_3$) [44], the following peak, above 400˚C, indicated the evolution from hematite to magnetite (Fe_3O_4) [45]. The manganite powder TGA curve (**Figure 4(c)**) presented four significant weight loss steps. The first one was small (about 1.4%) and occurred at 50˚C - 150˚C because of the surface water desorption [46]. The second one was observed between 160˚C - 340˚C (endothermic peak at 274.89˚C), indicating the structural conversion of $Mn^{3+}O$ (OH) into MnO_2. The third weight loss at 500˚C - 590˚C (endothermic peak at 437˚C) is associated to

the MnO_2 conversion into Mn_2O_3 [47]. Finally, the exothermic peak at 550˚C is due to a transition from Mn_2O_3 to well-crystallized α-MnO_2.

The zero point of charge of the as-synthesized materials were 9.2 for boehmite, 12.4 for goethite, and 2.2 for manganite, respectively. When the material is in an aqueous solution of pH = pH_{zpc} the charge of its surface is neutral; but if the pH > pH_{zpc} the surface is negatively charged and on the contrary, it is positively charged if pH < pH_{zpc}. Therefore, this parameter describes the variations in electric charge that are responsible for the interaction between the material surface and the ions present in aqueous solution and so designates the electrostatic affinity to anions or cations depending on the pH of the solution [48]. According to the results, boehmite and goethite will have affinity through the anion adsorption [49] [50]. In contrast, manganite is suitable for cation adsorption [51]. The results of the surface hydroxyl group content for the as-prepared materials (**Table 1**) show that goethite has the highest amount of hydroxyl groups per gram of material (1.7 meq OH^-/g), whereas the values for boehmite and manganite were 1.16 and 0.855 meq OH^-/g, respectively. The content of the hydroxyl group is considered as surface active sites for attracting ions in aqueous solution; thus, goethite has a large possibility of ion attraction on its surface.

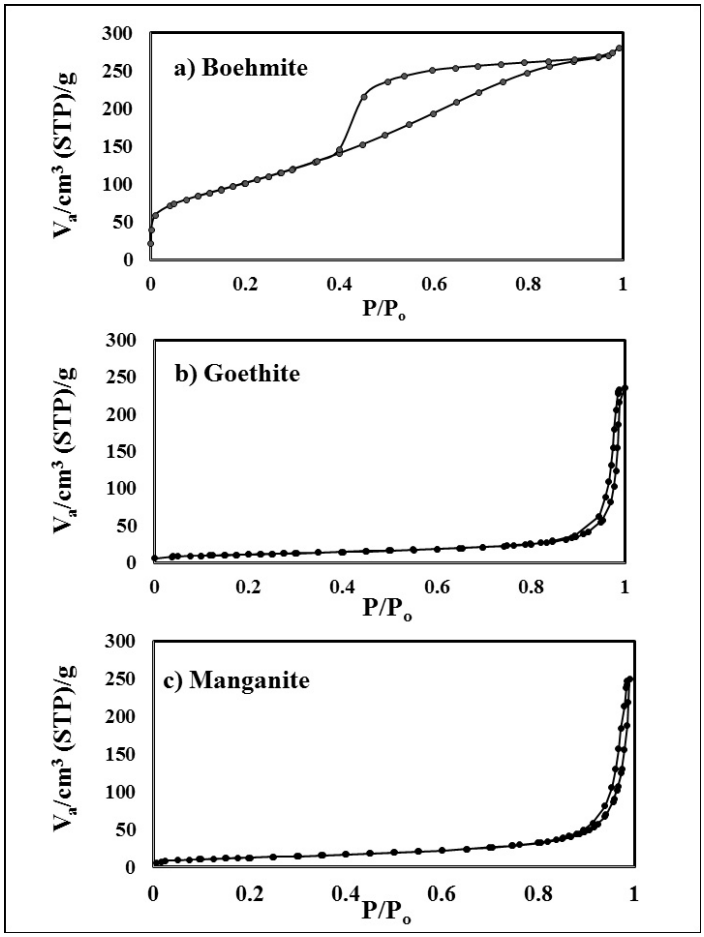

Figure 5. N_2 adsorption-desorption isotherms of as-prepared oxyhydroxides products.

Figure 5 shows the N_2 adsorption-desorption isotherms of the oxyhydroxides at 77 K. According to the International Union of Pure and Applied Chemistry (IUPAC), these materials presented type IV isotherms with hysteresis loop characteristic of mesoporous materials. The hysteresis of boehmite is larger than those corresponding to goethite and manganite. In general, these isotherm types are usually associated with materials in which monolayer-multilayer retention can occur.

Values of BET surface areas, mean pore diameters, and total pore volumes are in Table 1. These values are within those previously reported for materials synthesized in similar conditions than the present ones [52]; differences among the oxyhydroxides depend on the specific experimental conditions, like reaction times and temperature [27]. Values of the BET surface areas are bigger than 100 m^2/g indicating that the oxyhydroxides are not highly crystalline [53]. According to the mean pore diameters, these materials may be classified as mesoporous (2nm < size < 50 nm); interestingly, the values of goethite and manganite are very close, which may be due to the similarity of their methods of synthesis.

Table 1. Morphological characteristics pH_{zpc}, content of OH^- group, and surface fractal dimensions of the synthesized oxyhydroxides.

Parameter	Boehmite	Goethite	Manganite
BET surface area, m^2/g	380	413	188
Mean pore diameter, nm	4.6	34	33
Total pore volume, cm^3/g	0.43	0.34	0.38
V_m, cm^3	89.3	9.5	10.4
pH_{zpc}	9.2	12.3	2.2
Content of OH^- groups, meq/g	1.2	1.7	0.9
Surface fractal dimension	1.5	1.7	1.4

Data of a N_2 adsorption-desorption isotherms at 77 K were used to obtain the adsorbed volume (V), the relative pressure (P_o/P), and V_m values by means of the following equation (1):

$$\frac{P}{V\left(Po-P\right)}=\frac{1}{V_mC}+\frac{C-1}{V_mC}\left(\frac{P}{P_o}\right) \tag{1}$$

Values of the slope and the ordinate of a linear fit of data (Figures 6(a)-(c)) allow calculate V_m (Table 1). The corresponding to boehmite is higher than those to goethite and manganite. Next, Surface fractal dimensions D_f were calculated by the following equation (2) [6].

$$\ln\left(\frac{V}{V_m}\right)=cons\tan t+\frac{D_f-3}{3}\left[\ln\left(\ln\left(P_o/P\right)\right)\right] \tag{2}$$

A plot of $ln(V/V_m)$ as a function of $ln(ln\ (P_o/P)$, in a certain range (Figures 6(d)-(f)) gives a straight line and based on the slope the surface fractal dimension D_f was calculated. The values of the surface fractal dimensions of boehmite, goe-

thite and manganite are in Table 1. The magnitude of D_f may be used for the surface description of a material [54] and is associated with the surface active sites and with the functional groups like hydroxyl among others that are available for chemical, physical, or mechanical interaction with anions or cations in aqueous solutions [55]. Data of Table 1 reveals that the surface geometry of these oxyhydroxides are rather smooth at a molecular scale [56], *i.e.* their surfaces present scarce roughness.

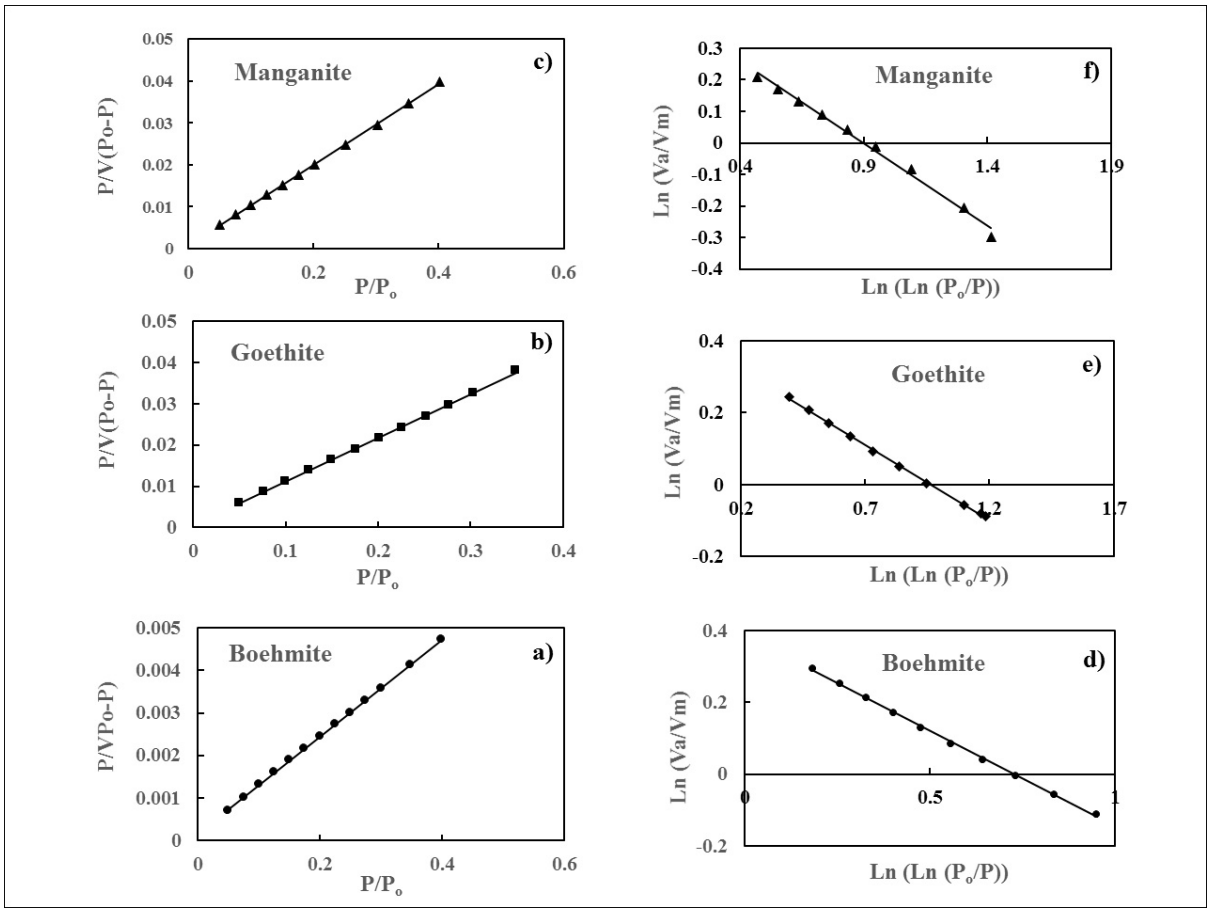

Figure 6. Plots for calculation of V_m, and surface fractal dimensions. (a) Boehmite $P/(V(P_o - P) = 0.011\ P/P_o + 0.0002$ (R^2 = 0.9999). (b) Goethite: $P/(V(P_o - P) = 0.106\ P/P_o + 0.0004$ (R^2 = 0.9994). (c) Manganite: $P/(V(P_o - P) = 0.097\ P/P_o + 0.0006$ (R^2 = 0.9997). (d) Boehmite: P/P_o range 1% - 22%; $\text{Ln}(V_a/V_m) = -0.51\ \text{Ln}\ (\text{Ln}\ (P/P_o)) + 0.37$ (R^2 = 0.9996). (e) Goethite: P/P_o range 4% - 25%; $\text{Ln}(V_a/V_m) = -0.42\ \text{Ln}\ (\text{Ln}\ (P/P_o)) + 0.4$ (R^2 = 0.9991). (f) Manganite: P/P_o range 2% - 20%; %; $\text{Ln}(V_a/V_m) = -0.52\ \text{Ln}\ (\text{Ln}\ (P/P_o)) + 0.44$ (R^2 = 0.9993).

Figure 7 displays a plot of hydroxyl group content as a function of the surface fractal dimensions, where linearity is observed. Ismail and Pfeifer (1994) [55] proposed a linear correlation between these parameters and the results obtained corroborate that proposal. The correlation between the active sites of a material directly depends on its roughness; the greater is this, the greater is the accessibility to the active sites. That property is very interesting in various processes, adsorption among others.

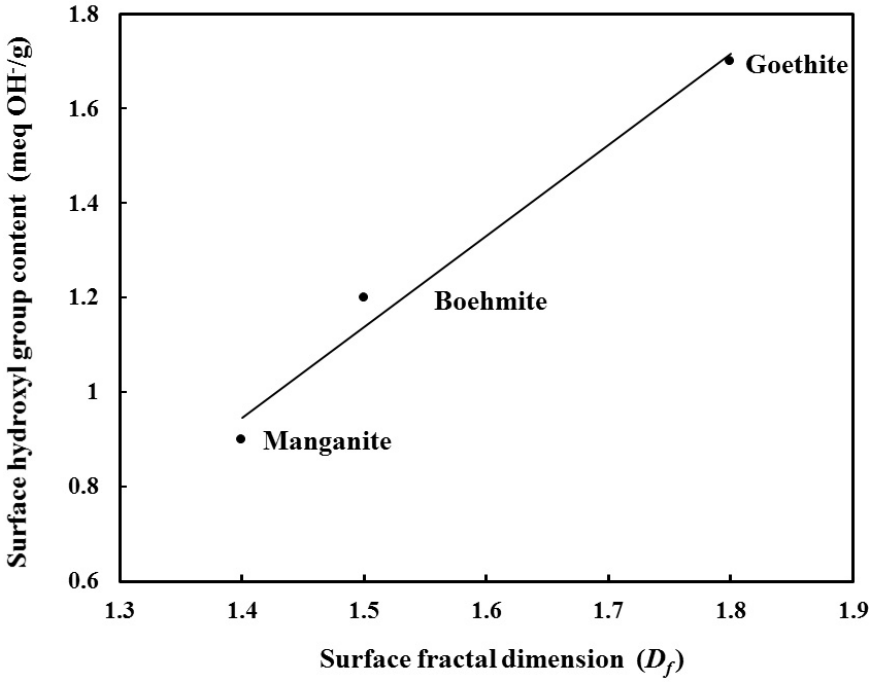

Figure 7. Surface hydroxyl group content *vs.* Surface fractal dimension. $D_f = 1.9\ [OH^-] - 1.7462$ ($R^2 = 0.98$).

4. Conclusion

In this study, boehmite, goethite, and manganite powders were successfully synthesized, having different structural, morphological, and textural characteristics. XRD patterns revealed that goethite, and manganite were of crystalline structure and boehmite was rather amorphous. These differences were then attributable to the preparation methods; those synthesized by chemical reactions were crystalline, while the sol-gel method resulted in a rather amorphous compound. TGA-DSC curves indicated that these oxyhydroxides undergo structural changes associated, initially with dehydroxylation into the range from 100˚C to 300˚C and thereafter to phase conversions between 400˚C and 600˚C. SEM-EDX showed that the as-prepared oxyhydroxide materials have particles of sizes between 10 to 400 μm. N_2 physisorption measurements and N_2 adsorption-desorption isotherms demonstrated that the materials are fine mesoporous powders with high BET surface areas (380, 413, and 188 m^2/g for boehmite, goethite, and manganite, respectively). Surface fractal dimensions showed that these materials were in the range from 1.4 to 1.7, indicating that their surfaces are lightly rough; the uniformity or dissimilarity of pore sizes depends on the grade of surface irregularity of the material. Interestingly the surface hydroxyl group content linearly correlated with the surface fractal dimensions. From which it is inferred that the greater the fractal dimension, and therefore the roughness of the material, the greater the possibility that the OH^- groups will be found on the surface. According to the zero point of charge concept, boehmite, and goethite have affinity for anions in aqueous media, whereas manganite, which showed a low value ($pH_{zpc} = 2.2$) may have preference

for cations. Therefore, the results indicate that the obtained materials possess different physicochemical characteristics for be used as effective adsorbents of contaminants in aqueous media.

Acknowledgements

The authors acknowledge the financial support of ININ (Project QU-001), and the technical assistance of Iris Zoet López-Malpica and Elvia Moreno-Morales.

Conflicts of Interest

The authors declare no conflicts of interest regarding the publication of this paper.

References

[1] Rajandran, P., Masngut, N., Manas, N.H.A., Azelee, N.I.W., Fuzi, S.F.Z.M. and Bunyamin, M.A.H. (2024) Fixed-bed Adsorption for Industrial Wastewater Purification: An In-Depth Review. *International Journal of Environmental Science and Technology*, **22**, 3943-3964. https://doi.org/10.1007/s13762-024-06034-4

[2] Hussain, M., Riaz, A., Zeb, H., Ali, A., Mujahid, R., Ahmad, F., *et al.* (2025) Paving the Path to Water Security: The Role of Advanced Adsorbents in Wastewater Treatment. *Journal of Water Process Engineering*, **71**, Article ID: 107333. https://doi.org/10.1016/j.jwpe.2025.107333

[3] Macena, M., Pereira, H., Cruz-Lopes, L., Grosche, L. and Esteves, B. (2025) Competitive Adsorption of Metal Ions by Lignocellulosic Materials: A Review of Applications, Mechanisms and Influencing Factors. *Separations*, **12**, Article 70. https://doi.org/10.3390/separations12030070

[4] Tamjidi, S., Moghadas, B.K., Esmaeili, H., Shakerian Khoo, F., Gholami, G. and Ghasemi, M. (2021) Improving the Surface Properties of Adsorbents by Surfactants and Their Role in the Removal of Toxic Metals from Wastewater: A Review Study. *Process Safety and Environmental Protection*, **148**, 775-795. https://doi.org/10.1016/j.psep.2021.02.003

[5] Zhan, H., Li, X., Hu, Z., Chen, L., Shen, W., Guo, W., *et al.* (2025) Effect of Particle Size on Pore Structure and Fractal Characteristics of Deep Siliceous Shales in Southern Sichuan, China, Measured Using Small-Angle Neutron Scattering and Low-Pressure Nitrogen Adsorption. *Fractal and Fractional*, **9**, Article 165. https://doi.org/10.3390/fractalfract9030165

[6] Pfeifer, P. (1988) Fractals in Surface Science: Scattering and Thermodynamics of Adsorbed Films. In: Vanselow, R. and Howe, R., Eds., *Chemistry and Physics of Solid Surfaces VII*, Springer, 283-305. https://doi.org/10.1007/978-3-642-73902-6_10

[7] Pfeifer, P. and Avnir, D. (1983) Chemistry in Noninteger Dimensions between Two and Three. I. Fractal Theory of Heterogeneous Surfaces. *The Journal of Chemical Physics*, **79**, 3558-3565. https://doi.org/10.1063/1.446210

[8] Martin, J.E., Schaefer, D.W. and Hurd, A.J. (1986) Fractal Geometry of Vapor-Phase Aggregates. *Physical Review A*, **33**, 3540-3543. https://doi.org/10.1103/physreva.33.3540

[9] Jaroniec, M. (1995) Evaluation of the Fractal Dimension from a Single Adsorption Isotherm. *Langmuir*, **11**, 2316-2317. https://doi.org/10.1021/la00006a076

[10] Tomchuk, O.V. (2020) The Concept of Fractals in the Structural Analysis of Nanosystems: A Retrospective Look and Prospects. *Ukrainian Journal of Physics*, **65**, 709.

https://doi.org/10.15407/ujpe65.8.709

[11] Rodríguez-Cuadrado, J. and San Martín, J. (2022) Shielding Material Distributions and Associated Fractals. *Chaos, Solitons & Fractals*, **158**, Article ID: 112008. https://doi.org/10.1016/j.chaos.2022.112008

[12] Tang, S., Huang, J., Duan, L., Yu, P. and Chen, E. (2020) A Review on Fractal Footprint of Cement-Based Materials. *Powder Technology*, **370**, 237-250. https://doi.org/10.1016/j.powtec.2020.05.065

[13] Li, L., Li, Z., Cao, M., Tang, Y. and Zhang, Z. (2021) Nanoindentation and Porosity Fractal Dimension of Calcium Carbonate Whisker Reinforced Cement Paste after Elevated Temperatures (UP to 900℃). *Fractals*, **29**, Article ID: 2140001. https://doi.org/10.1142/s0218348x21400016

[14] Yang, X., Li, L., Dai, H. and Jia, M. (2021) Effect of Fractal Dimension in Concrete Meso-Structure on Its Axial Mechanical Behavior: A Numerical Case Study. *Fractals*, **29**, Article ID: 2140011. https://doi.org/10.1142/s0218348x21400119

[15] Wang, L., Zeng, X., Yang, H., Lv, X., Guo, F., Shi, Y., *et al.* (2021) Investigation and Application of Fractal Theory in Cement-Based Materials: A Review. *Fractal and Fractional*, **5**, Article 247. https://doi.org/10.3390/fractalfract5040247

[16] Wang, L., Lu, X., Liu, L., Xiao, J., Zhang, G., Guo, F., *et al.* (2022) Influence of MgO on the Hydration and Shrinkage Behavior of Low Heat Portland Cement-Based Materials via Pore Structural and Fractal Analysis. *Fractal and Fractional*, **6**, Article 40. https://doi.org/10.3390/fractalfract6010040

[17] Farin, D. and Avnir, D. (1989) The Effects of the Fractal Geometry of Surfaces on the Adsorption Conformation of Polymers at Monolayer Coverage Part I. The Case of Polystyrene. *Colloids and Surfaces*, **37**, 155-170. https://doi.org/10.1016/0166-6622(89)80115-5

[18] Contreras-Ruiz, J.C., Martínez-Gallegos, M.S. and Ordoñez-Regil, E. (2016) Surface Fractal Dimension of Composites TiO_2-Hydrotalcite. *Materials Characterization*, **121**, 17-22. https://doi.org/10.1016/j.matchar.2016.09.032

[19] Vilchis-Granados, J., Granados-Correa, F. and Barrera-Díaz, C.E. (2013) Surface Fractal Dimensions and Textural Properties of Mesoporous Alkaline-Earth Hydroxyapatites. *Applied Surface Science*, **279**, 97-102. https://doi.org/10.1016/j.apsusc.2013.04.042

[20] Alvarado-Ibarra, Y., Granados-Correa, F., Lara, V.H., Bosch, P. and Bulbulian, S. (2009) Nickel (II) Sorption on Porous ZnO Prepared by Solution Combustion Method. *Colloids and Surfaces A*: *Physicochemical and Engineering Aspects*, **345**, 135-140. https://doi.org/10.1016/j.colsurfa.2009.04.045

[21] Dong, X., Zhang, X., Liu, B., Wang, H., Li, Y., Huang, Y., *et al.* (2006) Controlled Synthesis of Manganese Oxohydroxide (MnOOH) and Mn_3O_4 Nanorods Using Novel Reverse Micelles. *Journal of Nanoscience and Nanotechnology*, **6**, 818-822. https://doi.org/10.1166/jnn.2006.115

[22] Okada, K., Nagashima, T., Kameshima, Y., Yasumori, A. and Tsukada, T. (2002) Relationship between Formation Conditions, Properties, and Crystallite Size of Boehmite. *Journal of Colloid and Interface Science*, **253**, 308-314. https://doi.org/10.1006/jcis.2002.8535

[23] Inoue, K., Kwon, S., Suzuki, S., Saito, M. and Waseda, Y. (2006) Atomic-Scale Structure and Morphology of Ferric Oxyhydroxides Formed by Corrosion of an Iron-Silicon Alloy. *Materials Transactions*, **47**, 243-246. https://doi.org/10.2320/matertrans.47.243

[24] Crisostomo, V.M.B., Ngala, J.K., Alia, S., Dobley, A., Morein, C., Chen, C., *et al.*

(2007) New Synthetic Route, Characterization, and Electrocatalytic Activity of Nanosized Manganite. *Chemistry of Materials*, **19**, 1832-1839. https://doi.org/10.1021/cm062871z

[25] Liu, X., Qiu, G., Yan, A., Wang, Z. and Li, X. (2007) Hydrothermal Synthesis and Characterization of α-FeOOH and α-Fe_2O_3 Uniform Nanocrystallines. *Journal of Alloys and Compounds*, **433**, 216-220. https://doi.org/10.1016/j.jallcom.2006.06.029

[26] Swedlund, P.J., Webster, J.G. and Miskelly, G.M. (2009) Goethite Adsorption of Cu(II), Pb(II), Cd(II), and Zn(II) in the Presence of Sulfate: Properties of the Ternary Complex. *Geochimica et Cosmochimica Acta*, **73**, 1548-1562. https://doi.org/10.1016/j.gca.2008.12.007

[27] Granados-Correa, F., Corral-Capulin, N.G., Olguín, M.T. and Acosta-León, C.E. (2011) Comparison of the Cd(II) Adsorption Processes between Boehmite (γ-AlOOH) and Goethite (α-FeOOH). *Chemical Engineering Journal*, **171**, 1027-1034. https://doi.org/10.1016/j.cej.2011.04.055

[28] Wang, X., He, M., Lin, C., Gao, Y. and Zheng, L. (2012) Antimony(III) Oxidation and Antimony(V) Adsorption Reactions on Synthetic Manganite. *Geochemistry*, **72**, 41-47. https://doi.org/10.1016/j.chemer.2012.02.002

[29] Vázquez, A., López, T., Gómez, R., Bokhimi, Morales, A. and Novaro, O. (1997) X-ray Diffraction, FTIR, and NMR Characterization of Sol-Gel Alumina Doped with Lanthanum and Cerium. *Journal of Solid State Chemistry*, **128**, 161-168. https://doi.org/10.1006/jssc.1996.7135

[30] Boumaza, A., Favaro, L., Lédion, J., Sattonnay, G., Brubach, J.B., Berthet, P., *et al.* (2009) Transition Alumina Phases Induced by Heat Treatment of Boehmite: An X-Ray Diffraction and Infrared Spectroscopy Study. *Journal of Solid State Chemistry*, **182**, 1171-1176. https://doi.org/10.1016/j.jssc.2009.02.006

[31] Giovanoli, R. and Leuenberger, U. (1969) Über die Oxydation von Manganoxidhydroxid. *Helvetica Chimica Acta*, **52**, 2333-2347. https://doi.org/10.1002/hlca.19690520815

[32] Tanada, S., Kabayama, M., Kawasaki, N., Sakiyama, T., Nakamura, T., Araki, M., *et al.* (2003) Removal of Phosphate by Aluminum Oxide Hydroxide. *Journal of Colloid and Interface Science*, **257**, 135-140. https://doi.org/10.1016/s0021-9797(02)00008-5

[33] Kosmulski, M. (2004) pH-Dependent Surface Charging and Points of Zero Charge II. Update. *Journal of Colloid and Interface Science*, **275**, 214-224. https://doi.org/10.1016/j.jcis.2004.02.029

[34] Granados-Correa, F. and Jiménez-Becerril, J. (2009) Chromium (VI) Adsorption on Boehmite. *Journal of Hazardous Materials*, **162**, 1178-1184. https://doi.org/10.1016/j.jhazmat.2008.06.002

[35] Brigante, M., Zanini, G. and Avena, M. (2010) Effect of Humic Acids on the Adsorption of Paraquat by Goethite. *Journal of Hazardous Materials*, **184**, 241-247. https://doi.org/10.1016/j.jhazmat.2010.08.028

[36] Chen, W., Wang, N., Liu, L., Cui, Y., Cao, X., Chen, Q., *et al.* (2009) Facile Synthesis of Manganite Nanowires: Phase Transitions and Their Electrocatalysis Performance. *Nanotechnology*, **20**, Article ID: 445601. https://doi.org/10.1088/0957-4484/20/44/445601

[37] Li, F., Wu, J., Qin, Q., Li, Z. and Huang, X. (2010) Facile Synthesis of γ-MnOOH Micro/Nanorods and Their Conversion to β-MnO_2, Mn_3O_4. *Journal of Alloys and Compounds*, **492**, 339-346. https://doi.org/10.1016/j.jallcom.2009.11.089

[38] Ghosh, M.K., Poinern, G.E.J., Issa, T.B. and Singh, P. (2011) Arsenic Adsorption on Goethite Nanoparticles Produced through Hydrazine Sulfate Assisted Synthesis Method.

Korean Journal of Chemical Engineering, **29**, 95-102. https://doi.org/10.1007/s11814-011-0137-y

[39] Teoh, G.L., Liew, K.Y. and Mahmood, W.A.K. (2007) Synthesis and Characterization of Sol-Gel Alumina Nanofibers. *Journal of Sol-Gel Science and Technology*, **44**, 177-186. https://doi.org/10.1007/s10971-007-1631-x

[40] Kim, S., Lee, Y., Jun, K., Park, J. and Potdar, H.S. (2007) Synthesis of Thermo-Stable High Surface Area Alumina Powder from Sol-Gel Derived Boehmite. *Materials Chemistry and Physics*, **104**, 56-61. https://doi.org/10.1016/j.matchemphys.2007.02.044

[41] Betancur, J.D., Barrero, C.A., Greneche, J.M. and Goya, G.F. (2004) The Effect of Water Content on the Magnetic and Structural Properties of Goethite. *Journal of Alloys and Compounds*, **369**, 247-251. https://doi.org/10.1016/j.jallcom.2003.09.046

[42] Chen, X.Y., Zhang, Z.J., Li, X.L. and Lee, S.W. (2008) Controlled Hydrothermal Synthesis of Colloidal Boehmite (γ-AlOOH) Nanorods and Nanoflakes and Their Conversion into γ-Al_2O_3 Nanocrystals. *Solid State Communications*, **145**, 368-373. https://doi.org/10.1016/j.ssc.2007.11.033

[43] Rădițoiu, V., Diamandescu, L., Cosmin Corobea, M., Rădițoiu, A., Popescu-Pogrion, N. and Andi Nicolae, C. (2012) A Facile Hydrothermal Route for the Synthesis of α-FeOOH with Controlled Morphology. *Journal of Crystal Growth*, **348**, 40-46. https://doi.org/10.1016/j.jcrysgro.2012.03.032

[44] Chen, Y.H. (2013) Thermal Properties of Nanocrystalline Goethite, Magnetite, and Maghemite. *Journal of Alloys and Compounds*, **553**, 194-198. https://doi.org/10.1016/j.jallcom.2012.11.102

[45] Yuan, Z., Ren, T., Du, G. and Su, B. (2005) Facile Preparation of Single-Crystalline Nanowires of γMnOOH and $\beta$$MnO_2$. *Applied Physics A*, **80**, 743-747. https://doi.org/10.1007/s00339-004-3131-y

[46] Gao, T., Norby, P., Krumeich, F., Okamoto, H., Nesper, R. and Fjellvåg, H. (2009) Synthesis and Properties of Layered-Structured Mn_5O_8 Nanorods. *The Journal of Physical Chemistry C*, **114**, 922-928. https://doi.org/10.1021/jp9097606

[47] Kosmulski, M., Durand-Vidal, S., Mączka, E. and Rosenholm, J.B. (2004) Morphology of Synthetic Goethite Particles. *Journal of Colloid and Interface Science*, **271**, 261-269. https://doi.org/10.1016/j.jcis.2003.10.032

[48] Islam, M.A., Angove, M.J., Morton, D.W., Pramanik, B.K. and Awual, M.R. (2020) A Mechanistic Approach of Chromium (VI) Adsorption onto Manganese Oxides and Boehmite. *Journal of Environmental Chemical Engineering*, **8**, Article ID: 103515. https://doi.org/10.1016/j.jece.2019.103515

[49] Hongshao, Z. and Stanforth, R. (2001) Competitive Adsorption of Phosphate and Arsenate on Goethite. *Environmental Science & Technology*, **35**, 4753-4757. https://doi.org/10.1021/es010890y

[50] Pan, G., Qin, Y., Li, X., Hu, T., Wu, Z. and Xie, Y. (2004) EXAFS Studies on Adsorption-desorption Reversibility at Manganese Oxides-Water Interfaces: I. Irreversible Adsorption of Zinc onto Manganite (γ-MnOOH). *Journal of Colloid and Interface Science*, **271**, 28-34. https://doi.org/10.1016/j.jcis.2003.11.028

[51] Bochatay, L., Persson, P. and Sjöberg, S. (2000) Metal Ion Coordination at the Water-Manganite (γ-MnOOH) Interface: I. An EXAFS Study of Cadmium (II). *Journal of Colloid and Interface Science*, **229**, 584-592. https://doi.org/10.1006/jcis.2000.7013

[52] Paglia, G., Buckley, C.E., Udovic, T.J., Rohl, A.L., Jones, F., Maitland, C.F., *et al.* (2004) Boehmite-Derived γ-Alumina System. 2. Consideration of Hydrogen and Surface Effects. *Chemistry of Materials*, **16**, 1914-1923. https://doi.org/10.1021/cm035193e

[53] Pernyeszi, T. and Dékány, I. (2003) Surface Fractal and Structural Properties of Layered Clay Minerals Monitored by Small-Angle X-Ray Scattering and Low-Temperature Nitrogen Adsorption Experiments. *Colloid and Polymer Science*, **281**, 73-78. https://doi.org/10.1007/s00396-002-0758-0

[54] Avnir, D., Farin, D. and Pfeifer, P. (1985) Surface Geometric Irregularity of Particulate Materials: The Fractal Approach. *Journal of Colloid and Interface Science*, **103**, 112-123. https://doi.org/10.1016/0021-9797(85)90082-7

[55] Ismail, I.M.K. and Pfeifer, P. (1994) Fractal Analysis and Surface Roughness of Nonporous Carbon Fibers and Carbon Blacks. *Langmuir*, **10**, 1532-1538. https://doi.org/10.1021/la00017a035

[56] Raoufi, D., Kiasatpour, A., Fallah, H.R. and Rozatian, A.S.H. (2007) Surface Characterization and Microstructure of ITO Thin Films at Different Annealing Temperatures. *Applied Surface Science*, **253**, 9085-9090. https://doi.org/10.1016/j.apsusc.2007.05.032